Agricultural Water Management 129 (2013) 200–211

Contents lists available at ScienceDirect

Agricultural Water Management

journal homepage: www.elsevier.com/locate/agwat

Control of atmospheric fluxes from a pecan orchard by physiology, meteorology, and canopy structure: Modeling and measurement

Vincent P. Gutschick[a,*], Zhuping Sheng[b]

[a] Global Change Consulting Consortium, Inc., 4904 Calabazilla Drive, Las Cruces, NM 88011, USA
[b] Texas AgriLife Research Center at El Paso, Department of Biological and Agricultural Engineering, TAMU, 1380 A&M Circle, El Paso, TX 79927, USA

ARTICLE INFO

Article history:
Received 8 November 2012
Received in revised form 13 July 2013
Accepted 1 August 2013
Available online 30 August 2013

Keywords:
Pecan
Evapotranspiration
Process model
Eddy covariance
Control
Humidity response
Parametrization

ABSTRACT

We constructed and validated against eddy-covariance data a model of the fluxes of water vapor, sensible heat, CO_2, and radiation in a substantially mature pecan orchard (*Carya illinoinensis* (Wangenh.)K. Koch) in an arid environment near El Paso, TX, USA. The detailed process-based model is designed for insights into major control points for photosynthetic gain and water use as exerted by canopy structure, leaf physiology, and micrometeorological drivers. Toward this end, it resolves extensive details of leaf micro environments (radiation and scalars) in realistic canopy structures, as well as photosynthetic and respiratory physiology, stomatal control, and water relations from roots to leaves. The model is for a static mid-season canopy, with the ability to link it to dynamics models of development and management. Field flux measurements agreed well with model estimates that were derived using measurable parameters rather than data-fitting. An exception was the measurement-model disparity in sensible heat flux under conditions of strong advection of dry air; the model diagnostics imply a marked insensitivity of pecan stomata to humidity that has not been reported earlier. Formulation and parametrization of most of the physical and physiological processes was robust, shared well between the study site and an alternate site, but gaps are evident in the knowledge of several important processes, primarily in responses to water stress. The study indicates limitations in simpler models, such as those based on constant canopy conductance or light-use efficiency, while offering leads to making more accurate simple models suitable for use in decision support systems, ultimately for stress management under limited water availability.

1. Introduction

Agricultural water management faces challenges at multiple scales, from growers to water authorities. On a global scale, irrigation shortfalls are expected to increase (Wada et al., 2012), with water shortages extending to other, competing consumptive uses (Vörösmarty et al., 2010). Some of the challenges may be addressed with optimal irrigation methods on farms and in orchards. Irrigation scheduling to avoid stress (e.g., Miyamoto, 1984; Kallestad et al., 2006) is one element. Optimization of stress levels to limit yield reductions and improve water-use efficiency is another element, having been explored primarily under the rubric of deficit irrigation (DI; Behboudian and Mills, 1997) and related but not equivalent partial root drying (Fernandez et al., 2006; Romero et al., 2005). For tree nut crops such as we focus upon, DI has been studied (pistachio, *Pistacia vera* L: Gijon et al., 2009; Goldhamer and Fereres, 2004; Romero et al., 2005; Shackel et al., 2000). However, the detailed physiological basis of stress responses has not been elucidated; experiments remain empirical, with intuition dominating over physiological process knowledge. Process-based models afford the opportunity to integrate extant knowledge while highlighting the limitations of such knowledge for productive research direction. Provided that the known processes are formulated with robust models, model simulations enable the identification of a small suite of most informative experiments, reducing the research effort. By "robust models," we mean models that have been comprehensively tested and that have ready or, best of all, nearly universal parameterization, such as the photosynthesis model of Farquhar et al. (1980). Such reduction of the scope of experiments is particularly merited in studies of stress. Long-lived woody crops are valuable, and growers rarely are willing to risk their investment on experiments, and then only with a deep justification. Once tested, process-based models also can be applied in new locations and climates with notably better confidence than with empirical or statistical models.

Of course, complex process-based models must be reduced to simpler models for application by farmers, growers, and water managers. A simpler model is then profitably incorporated into a user-friendly interface that allows the specification of management

* Corresponding author. Tel.: +1 575 571 2269; fax: +1 575 646 5665.
E-mail addresses: vince@gcconsortium.com, vince.gutschick@gmail.com (V.P. Gutschick), z-sheng@tamu.edu (Z. Sheng).

0378-3774/$ – see front matter © 2013 Elsevier B.V. All rights reserved.
http://dx.doi.org/10.1016/j.agwat.2013.08.004

options. The resultant decision support system (DSS) must also provide predicted results such as yield in a compact, comprehensible manner. It is also valuable for the DSS to provide key diagnostics of intermediate results (water status, etc.) that can be checked in the field. Making a useful DSS is fraught with pitfalls (Matthews et al., 2008), as is even the development of the complex base model (Johnson, 2011; Vogel et al., 1995), but a great variety of DSSs have been developed; a search on "decision support system" "agriculture" returned 174 results. For example, the DSSs for soybean (*Glycine max* (L.) Merr.) (SOYGRO; original reference Wilkerson et al., 1983) and cotton (*Gossypium hirsutum* L.) (GOSSYM; original reference Fye et al., 1981) have been used for many years.

The trajectory of developing a comprehensive model, then simpler models that are locally parametrized, and finally a DSS, is mandated not by computational demand but by the need to reduce "data hunger" for the ultimate users. Current levels of computational power and of mathematical methods make the execution of extremely large models practical on short time scales. However, complex agricultural models generally involve specification of many parameters for crop physiology, soil properties, and crop structure, – more than growers and farmers can afford to measure as model inputs. DSS developers then bear the burden of projecting complex models to simpler forms. In this task, they can apply knowledge of the patterns of parameters over wide geographic regions, climates, soils, and crop varieties. More to the point of the current effort, the developers can identify robust process descriptions to use in simpler models. We have cited above the photosynthesis model of Farquhar et al. (1980), and there is evidence that stomatal control models originating with the model of Ball et al. (1987) are robust. Using complex models such as we present here can aid in discovering more such robust descriptions. Another utility of complex models is discovering the parameters to which crop performance is most sensitive, thus, the parameters for which accurate measurement is most necessary.

The current study presents a model for whole-orchard energy fluxes and photosynthesis, as well as the justifications for decisions on its structure. The model is intended to be a major step in developing a decision support system, as well as to aid the development of better crop models of diverse physiological, biophysical, and meteorological processes at suitable levels of detail for each process. It will be incorporated into a larger modeling framework, comparable to that presented in previous work (Andales et al., 2006). The simulations are tested against flux measurements by eddy covariance, as well as for internal consistency.

2. Materials and methods

2.1. The model

2.1.1. Basic structure

The model computes and sums fluxes of water vapor, heat, and CO_2 on an hourly basis from individual leaves, sampled at a selectable number of locations within the crown of a central tree as steps in radius, zenith, and azimuth. Leaves are also sampled at a finite number of angular orientations. A uniform leaf angle distribution in zenith and azimuth is assumed (Ross, 1981). A user of the model specifies orchard structure that affects light interception, specifying for the central tree and an arbitrary number of neighboring trees in rows and columns each tree's location (centroid Cartesian coordinates) and its crown geometry as an ellipsoid of revolution (major and minor axis dimensions and zenith and azimuthal angles of the major axis tilt). All crowns are modeled as having a uniform foliage density, f_d, throughout their volume. The fluxes of water vapor, heat, and CO_2 at a central tree are taken as representative of the whole orchard, and they are subsequently scaled to fluxes per unit ground area for comparison with eddy-covariance data. The parameters and variables in the model are summarized in Table 1.

The model currently does not resolve latent and sensible heat fluxes at the soil, canopy rainfall interception or dewfall, or transients in photosynthetic fluxes from varying light levels. The model uses a static canopy structure as a useful approximation for important midseason performance.

The model is coded in Fortran 90 with extensive commenting. Variables are all of explicitly declared type, with descriptions of their meaning and their physical units. The code and sample input data and output files are available online at http://gcconsortium.com/pecan/pecan_model.pdf and at http://pecanmodel.blogspot.com/p/model-version-2012-05-14.html.

2.1.2. Leaf properties and processes

Leaf linear dimension, d_{leaf}, crosswise to the midrib, is specified for computing the convective heat transfer. Leaves are described, first, by their optical properties (absorbances in the wavebands of photosynthetically active radiation [PAR] and near-infrared radiation [NIR] and corresponding transmittances). Second, their photosynthetic physiology is described within the robust model of Farquhar et al. (1980), by: maximal carboxylation capacity ($V_{c,max}^{25}$, light- and CO_2-saturated); CO_2 and O_2 binding constants K_C and K_O; photorespiratory offset Γ^*; initial quantum yield at CO_2-saturation Q_0; the transition parameter θ_{PS} between light-limited and light-saturated regimes; and the standard temperature dependences of these quantities. Photosynthetic limitations posed by electron transport or triose-phosphate transport are not accounted, as they are commonly significant only at elevated CO_2 levels. Employing a simplification (linearization) of the empirical studies of Niinemets (2007), maximal photosynthetic capacity is modeled as linearly proportional to mean PAR irradiance at each canopy location, with a nonzero intercept (Lombardini et al., 2009). The mean PAR irradiance is evaluated on a user-specified day, chosen as typical of the season. Third, the leaf basal respiration rate is specified at the mean photoperiod temperature, T_{mean}, of the preceding two weeks, to which this respiration has acclimated (Wythers et al., 2005). Respiration at other temperatures is scaled by the factor $exp(0.07^*[T_{leaf}–T_{mean}]$, where T_{leaf} is the leaf temperature). The basal leaf respiration rate is scaled at each canopy location as directly proportional to the value of photosynthetic capacity at that location. The stomatal control program is formulated in standard Ball–Berry form (Ball et al., 1987) for stomatal conductance, $g_s = m_{BB} A\, h_s/C_s + b_{BB}$. Here, the slope, m_{BB}, and the intercept, b_{BB}, are fixed parameters, A is the leaf photosynthetic rate, and h_s and C_s, are relative humidity and CO_2 mixing ratio at the leaf surface. Two options switches described in the Results and Discussion allow the user to apply an exponent other than unity to the surface relative humidity, h_s, and to use either net or gross leaf photosynthesis. Newer alternative formulations (Leuning, 1995; Dewar, 2002) were found to give slightly poorer fits to leaf gas-exchange data on other pecan trees (Johnson, 2004).

2.1.3. Projection of microenvironment to the leaf level

Weather data are taken from a weather station location 1.2 km to the southeast of the eddy-covariance tower. Humidity and temperature within the canopy are taken as uniform at all leaves, as in common two-layer models, while being modified from free-air values by canopy self-humidification and self-heating. Consequently, water vapor pressure in the air within the canopy, $e_{air,can}$, is modeled as $e_{air,can} = e_{air} + E\,P_{air} r_a = e_{air} + E\,P_{air}/g_a$, where: e_{air} (in Pa) is the free-air value at the weather station; E is the transpiration flux density per unit ground area in units of mol m^{-2} s^{-1}; P_{air} is total air pressure in Pa; and r_a is the canopy aerodynamic resistance, $1/g_a$, also in molar units. The value of aerodynamic conductance, g_a (in

Table 1
Symbols used in the text.

Symbol	Meaning	Units
A or A_{leaf}	Leaf photosynthetic rate	$mol_{CO2}\ m^{-2}\ s^{-1}$
A_{can}	Net CO_2 flux from canopy	$mol_{CO2}\ m^{-2}\ s^{-1}$
a_{PAR}	Leaf absorptivity in the PAR	(-)
A_{tree}	Whole tree photosynthetic rate	$kg_{photosynthate}\ h^{-1}$
b_{BB}	Intercept in Ball–Berry model of stomatal conductance	$mol\ m^{-2}\ s^{-1}$
C_1	Coefficient of aerodynamic resistance	(-)
C_P	Molar heat capacity of air	$J\ mol^{-1}\ K^{-1}$
C_s	CO_2 mixing ratio at leaf surface	(-)
d_{tree}	Spacing between trees	m
d_{leaf}	Leaf linear dimension	m
E	Transpiration flux density per unit ground area	$mol_w\ m^{-2}\ s^{-1}$
e_{air}	Partial pressure of water vapor in free air	Pa
$e_{air,can}$	Partial pressure of water vapor inside the canopy	Pa
E_{leaf}	Leaf transpiration rate	$mol_w\ m^{-2}\ s^{-1}$
E_{tree}	Whole-tree transpiration rate	$L\ h^{-1}$
ET	Evapotranspiration rate	$mm\ d^{-1}$
f_d	Foliage density	$m^2\ m^{-3} = m^{-1}$
g_a	Canopy aerodynamic conductance, molar units	$mol\ m^{-2}\ s^{-1}$
g_{can}	Whole-tree conductance for water vapor	$mol_w\ m^{-2}\ s^{-1}$
$g_{leaf,H}$	Boundary-layer conductance of leaf for sensible heat	$W\ m^{-2}\ K^{-1}$
g_s	Leaf stomatal conductance for water vapor	$mol_w\ m^{-2}\ s^{-1}$
$g_{tot,leaf}$	Total stomatal + boundary-layer conductance of leaf for water vapor	$mol_w\ m^{-2}\ s^{-1}$
H	Sensible heat flux density	$W\ m^{-2}$
h_s	Relative humidity at leaf surface	(-)
I	Irradiance on leaf	$mol_{photons}\ m^{-2}\ s^{-1}$
K_C	Binding constant for CO_2 at Rubisco	Pa
K_O	Binding constant for O_2 at Rubisco	Pa
L	Leaf area index along ray path	$m^2\ m^{-2}$ (-)
LE	Latent heat flux density	$W\ m^{-2}$
LUE	Light-use efficiency, quantum	$mol_{CO2}\ mol_{photons}^{-1}$
m_{BB}	Slope in Ball–Berry model of stomatal conductance	(-)
P_{air}	Total air pressure	Pa
P_{pen}	Penetration probability of direct solar beam	(-)
$P_{pen,diff}$	Penetration probability of diffuse radiation	(-)
Q_0	Initial quantum yield at CO_2-saturation	$mol_{CO2}\ mol_{photons}^{-1}$
Q_{sol}	Total shortwave radiant energy flux density	$W\ m^{-2}$
R	Radius of tree crown	m
r_a	Aerodynamic canopy resistance, molar units	$mol^{-1}\ m^2\ s$
R_{bulk}	"Bulk" respiration rate per ground area	$mol_{CO2}\ m^{-2}\ s^{-1}$
$T_{air,abs}$	Air temperature, absolute	K
$T_{air,can}$	Air temperature within canopy	°C
$T_{leaf,mean}$	Mean leaf temperature in canopy	°C
T_{mean}	Mean leaf temperature in photoperiod, past 2 weeks	°C
u	Windspeed in free air	$m\ s^{-1}$
$V_{c,max}{}^{25}$	Maximal carboxylation capacity of leaf at 25 °C	$mol_{CO2}\ m^{-2}\ s^{-1}$
VPD	Vapor pressure deficit	Pa
β	Stomatal responsiveness to root water potential	MPa^{-1}
Γ^*	"Photorespiratory" offset in enzyme-kinetic photosynthetic rate	Pa
δ	Stomatal responsiveness to leaf water potential	MPa^{-1}
ε_{sky}	Effective thermal emissivity of sky	(-)
ρ_{air}	Molar density of air	$mol\ m^{-3}$
θ_{PS}	Parameter for transition between light-limited and light-saturated photosynthetic rates	(-)
ψ_{leaf}	Leaf water potential	MPa
ψ_{root}	Root water potential	MPa
ψ_{soil}	Soil water potential	MPa

molar units, $mol\ m^{-2}\ s^{-1}$) is proportional to free-air wind speed, u, as $g_a = \rho_{air}\ u/C_1$, with C_1 as a constant that depends upon leaf area index (Sellers et al., 1996) and ρ_{air} as the molar density of air. A minimal value of $u = 1\ m\ s^{-1}$ is imposed to account roughly for free convection at low wind speeds. Similarly, air temperature within the canopy is offset, as $T_{air,can} = T_{air} + H/(C_P g_a)$, with H as the sensible heat flux density in $W\ m^{-2}$ and C_P as the molar heat capacity of air.

The radiation environment of leaves is specified in wavebands of PAR, NIR, and thermal infrared radiation (TIR); the small flux of ultraviolet radiation is ignored. The weather station provides only pyranometer data on total shortwave radiant energy density, Q_{sol}. The model estimates the partitioning of solar shortwave radiation into PAR and NIR and then into direct beam and diffuse flux densities, as described in the Appendix A, Part A1.

The direct beam (in PAR or NIR) is modeled as propagating to a given canopy location in the central tree with a penetration probability $P_{pen} = \exp(-0.5^* f_d\ L)$, with f_d again as foliage density and L as the total (segmented) path within crowns transited between the canopy location and the top of the canopy. Here, L is computed by ray-tracing in small, finite steps through the central-tree crown and all other crowns in the path. For a uniform leaf-angle distribution, there is then a uniform probability of leaf irradiance, $P_{pen}\ dI/I_0$, that leaf area has irradiance between I and $I + dI$, at any irradiance I, up to I_0, the maximal irradiance of the direct beam at normal incidence (Gutschick, 1991). Irradiance by diffuse light is estimated as the top-of-canopy flux density, D_0, multiplied by the fraction of diffuse radiation, $P_{pen,diff}$ reaching the canopy location. In turn, $P_{pen,diff}$ is estimated by ray-tracing from 25 sky directions, summing the probabilities and dividing by 25. Diffuse light is assumed to arrive

deterministically – that is, uniformly on leaves of any orientation (Gutschick, 1988) – and the irradiance is simply added to that from direct-beam irradiance.

Irradiance on leaves from light scattered from other leaves and the ground is estimated as being the same as in a uniform layered canopy (ULC) of the same mean leaf area index. The model computes absorbed fluxes at a large number of optical depths in a ULC, using a two-stream model of diffuse light propagation (compare Liang and Strahler, 1995, for a discussion, including limitations). The absorbed flux densities are then mapped onto locations in the real canopy by matching the values of mean direct-beam penetration probabilities. This is a simple heuristic model that has not been tested against a detailed radiative transfer model.

TIR irradiance at a canopy location is estimated as uniform diffuse radiation from the sky, arriving with a probability $P_{pen,diff}$ and uniform diffuse radiation from other leaves and soil, arriving with probability $1\text{-}P_{pen,diff}$. Flux density of sky radiation in the TIR waveband is estimated as $\varepsilon_{sky}\,\sigma\,T_{air,abs}{}^4$, with ε_{sky} as an effective sky emissivity computed from air temperature and humidity (Brutsaert, 1975), σ as the Stefan–Boltzmann constant, and $T_{air,abs}$ as the absolute temperature of air. Flux density of TIR from leaves and soil is estimated simply from the canopy leaf temperature using the analogous Stefan–Boltzmann form with an emissivity of unity.

Leaf temperature for each canopy location and leaf angular orientation is computed from basic energy-balance equations (e.g., Campbell and Norman, 1998), resolving interception of shortwave (PAR and NIR) and TIR radiation, TIR emission, evaporative cooling, and convective cooling. Steady state is assumed.

2.1.4. Water relations of leaves and stress responses

Leaf water potential, ψ_{leaf}, is taken as uniform throughout the canopy and is computed via a catenary, soil → root → leaf, with appropriate resistances in each link. The stem resistance between root and leaf is entered as a fixed parameter, independent of stress level for moderate stress (with no accounting for progressive or hysteretic cavitation in the stem, such as described by Cochard et al., 2002, or for temperature-dependence as described by Matzner and Comstock, 2001). The soil-to-root resistance is described with the basic model of Lafolie et al. (1991), with details given in the Appendix A, Part A2.

The effect of water stress on leaf function is modeled as a multiplicative factor of leaf and root (ψ_{root}) water potentials, $f_{gs} = \exp(\beta\,\psi_{root} + \delta\,\psi_{leaf}) < 1$, applied to the Ball–Berry form for stomatal conductance. This form is adapted from similar forms found useful in estimating responses of herbaceous plants (e.g., Tardieu and Simonneau, 1998). Stomatal control is intrinsically complex (Dewar, 2002; Buckley, 2005); reliable expressions for trees are rare (Cochard et al., 2002; Thomas and Eamus, 2002) and wholly lacking for orchard pecans. A specialized mathematical solution method is required to converge on a consistent solution for both whole-tree transpiration, E_{tree}, and whole-tree stomatal (plus boundary-layer) conductance, g_{can}; please see the Appendix A, Part A3.

No significant change in photosynthetic capacity is proposed at low to moderate water stress (Wilson et al., 2000). Respiration rates are not changed by stress; evidence of changes at high stress exists in some species (Ribas-Carbo et al., 2005), but measurements in pecans are lacking.

2.1.5. Soil and root water relations

Soil water content is modeled with a bucket model, homogeneous over a depth S. Soil water potential, ψ_{soil}, is computed with standard forms parametrized for the given soil texture class (van Genuchten, 1980; Hodnett and Tomasella, 2002). Hydraulic resistance from bulk soil to the (uniform) fine-root surface is computed with the model of Lafolie et al. (1991), with key parameters as soil texture class, soil depth, total fine root mass, and mean radius and dry-matter density of fine roots.

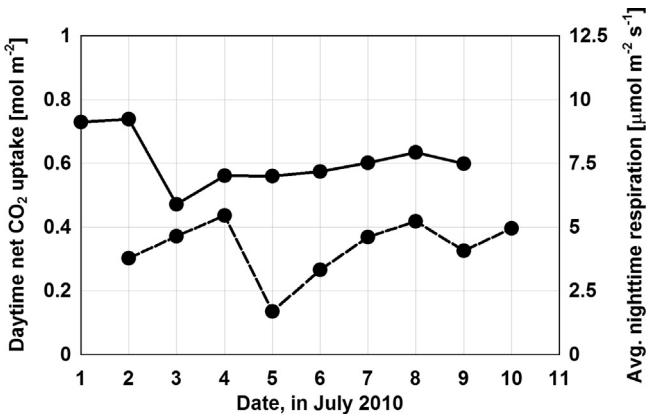

Fig. 1. Dark respiration rate scales as net photosynthesis summed over the complete photoperiod of the previous day, to the nearest half hour of eddy-covariance data.

2.1.6. Estimation of bulk respiratory contributions to CO_2 flux density

Within the model, leaf respiration is accounted, but the bulk of respiratory CO_2 flux arises from the stem, roots, and soil organisms. Thus, the net CO_2 flux, which we denote as A_{can} or J_{CO2}, measured by eddy covariance (EC), cannot be compared with the (nearly) gross flux computed by the model. Therefore, we compute the "bulk" respiration, R_{bulk}, outside the model and subtract it from the gross flux to estimate net flux.

Bulk respiration, R_{bulk}, appears to scale exponentially with temperature, as $R_{bulk} = R_{bulk}{}^0 \exp(0.07^*(T\text{–}T_{ref}))$, with T as the time-lagged temperature of the main compartments and T_{ref} as an arbitrary reference temperature. Such a formulation is argued concisely by Houborg et al. (2009). We impose a lag of minus four hours to account for delays in heat transfer. We estimate $R_{bulk}{}^0$ from night time fluxes. The value of $R_{bulk}{}^0$ appears to scale with the total daytime net CO_2 flux of two days prior to the night (Fig. 1). A limitation of this analysis is that nighttime CO_2 fluxes often occur at low wind speeds (low friction velocity, u^*) that generate smaller eddies not well sampled by EC (Barr et al., 2006). Other limitations arise from offsets generated by small-scale advection and storage changes.

2.1.7. Model parametrization

All parameters are derived from independent measurements on the canopy or similar canopies or trees. No fitting of curves has been done for the current study. We note that one objective of the current study is to determine which parameters are most strongly controlling for fluxes.

Tree spacing, 9 m, is set from direct measurements on the orchard. Individual tree crowns are approximated as uniform and spherical. Crown radius is determined from direct observation in the orchard, although it varies among subplots, as described in the results section. A mean cover fraction of 70%, also determined from aerial imagery, is consistent with a crown radius $R = 4.25$ m on a tree spacing $d_{tree} = 9$ m. Foliage density, $f_d = 0.65\ m^{-1}$ (as $m^2 m^{-3}$), is consistent with a measurement of $0.70\ m^{-1}$ in an older canopy via a LI-COR LAI-2000 canopy analyzer (LI-COR, Inc., Lincoln, NE, USA). It is also consistent with limited measurements of direct-beam penetration fraction to the ground within the crown projected area, averaging 16%. The calculation is given in the Appendix A, Part A4, along with a short note that whole-tree transpiration rates are only moderately sensitive to estimated foliage density (less strongly than as the square root). Leaf crosswise dimension of 0.05 m is typical of pecans, and results are minimally sensitive to this value.

Leaf and soil optical parameters: leaf absorptivity is estimated at 0.85 in the PAR (a_{PAR}) and 0.30 in the NIR (a_{NIR}). Leaf transmissivity is estimated as 0.05 in the PAR and 0.217 in the NIR. No detailed survey was performed in the orchard, but these values are consistent with detailed measurements on younger trees by Johnson (2004) and with a range of studies on other sun-adapted plants. Soil reflectivity is estimated as 0.30 in both PAR and NIR, without detailed measurements; results are not significantly sensitive to the values.

The Ball–Berry slope is set at $m_{BB} = 10$, the intercept at $b_{BB} = 0.02\ mol\ m^{-2}\ s^{-1}$, and the leaf carboxylation capacity, $V_{c,max}{}^{25,0}$ for topmost sunlit leaves at 100 μmol $m^{-2}\ s^{-1}$, based on a detailed reanalysis of gas-exchange measurements on similar trees in nearby Las Cruces, New Mexico, USA by Johnson (2004) for the same season in 2002 and 2003 and by Frias-Ramirez (2002) in October 1999. These values have significant uncertainty, given that the reanalysis gave wide ranges between sampling dates (see Appendix A, Part A5). No direct gas-exchange data have been obtained on the orchard studied in this report. The enzyme-kinetic parameters K_C, K_O, Γ^*, and Q_{00} were set from consensus values reported by Farquhar et al. (1980). The value of the parameter, θ_{PS}, for the transition from light-limited to light-saturated photosynthetic rates is set at 0.8, as found in a wide range of studies.

Most parameters for water stress are not relevant in the current study. Rather, they are included in the model for a subsequent estimate of stress responses. The values (Appendix A, Part A6) are consistent with measurements on pecans in nearby Las Cruces, NM, USA (Deb et al., 2011).

2.1.8. Mathematical methods and controls

A number of control parameters, settable by the user, address the number of canopy locations sampled, the number of leaf irradiance levels sampled, discretization stepsize for ray-tracing for light interception, the convergence criteria of iterations for leaf fluxes and whole-canopy fluxes, and output options.

The equations for stomatal conductance, energy balance, photosynthetic rate, and transport of CO_2 and water vapor all involve each other. The solution is iterative, using a novel scheme that is robust (Wang et al., 2007).

The code is presented in Supplementary Material, along with a narrative description and a flowchart, a sample input file, and several intermediate results of the calculations of more specialized interest to modelers.

2.1.9. Model outputs

The model runs on an hourly time scale and generates several output files. The principal file reports rates of transpiration, E_{tree}, and photosynthesis, A_{tree}, per tree and per unit ground area for each date and hour of the simulation as the key state variables. It also reports soil water content, soil and root water potentials, soil-to-root hydraulic resistance, the reduction factor for stomatal conductance from water stress, the free-air and in-canopy magnitudes of air temperature and water–vapor partial pressure, the number of iterations to converge the in-canopy conditions, and control coefficients. The control coefficient for stomatal conductance over transpiration, E, is posited as the relative change in E divided by the relative change in stomatal conductance, g_s, as $(\Delta E/E)/(\Delta g_s/g_s)$. To compute these changes, the model recomputes all processes with the same microenvironmental conditions at each crown location but with g_s reset to a value 10% larger. The end of the file presents total water use and photosynthate production over the simulation period and additional statistics.

Additional output files present (a) the daily-total fluxes of transpiration and photosynthesis; (b) for each day and hour, the canopy-mean values of leaf-to-air *VPD* and leaf temperature, both weighted by g_s, the whole-tree conductance (exclusive of the canopy boundary layer), and the mean values of leaf-surface relative humidity and leaf-internal CO_2 partial pressure, both of which are important in stomatal control and water-use efficiency; (c) histograms, among all leaf area, of PAR irradiance (with and without the inclusion of scattered light), leaf temperature (raw and also weighted by transpiration rate or photosynthetic rate), and stomatal conductance (with similar weighting options). The histograms are valuable in interpreting the relative importance of various processes, such as the contribution of shade leaves to fluxes or the contribution of scattered light to fluxes.

The model is composed of a large main program and 16 subroutines. The schema for calling is presented in the extensive comments at the beginning of the code.

2.2. Eddy covariance measurements of fluxes

2.2.1. Site description

The orchard of pecans, covering more than 400 ha on a 2 km by 4 km area, is located approximately 65 km southeast of El Paso, TX, USA, at latitude 31° 24′44.35″ N and longitude 106° 04′43.70″ W. The elevation is 1091.5 m. The trees, of variety Western, are planted in square patterns 30 feet (9 m) on a side, on soils that are variously Harkey loam and Harkey silty clay loam (thermic Typic Torrifluvent, Entisol). Ground cover is suppressed with mowing and herbicides. The trees vary in age, averaging 15 years. On average, the crowns cover 70% of the ground area, as determined by both ground surveys and image analysis on Google Earth satellite imagery. Cover varies from 60% to 86% along the octants as viewed from the eddy covariance tower. Mean tree height is approximately 10–11 m and has increased approximately 0.5 m annually; the eddy covariance anemometer system is adjusted annually to be approximately 2 m above the local mean canopy height. The flux footprint is estimated to within the minimal 1255 m distance to the orchard limit in any direction (Baldocchi, 1997; Schmid, 2002).

The orchard is irrigated with 75–100 mm of surface water diverted from the Rio Grande. Irrigation was approximately every 14 days, for 14 times within the year 2010. Irrigation dates are reported by the manager but are also indicated by soil moisture sensors at the tower location. Nitrogen fertilizer is applied four times annually at 75 kg/ha; records of leaf nitrogen content are not available.

2.2.2. Eddy-covariance instrumentation

Sensors are deployed on a triangular guyed tower 18 m in height. A 3-D sonic anemometer (CSAT3, Campbell Scientific, Logan, UT, USA) is coupled to an open-path CO_2/H_2O gas analyzer (LI-7500-TM, LI-COR Inc., Lincoln, NE, USA), with sampling at 60 Hz. Net radiation is measured with a REBS radiometer (Q-7.1, Campbell Scientific). At the tower location, soil water content is measured by a reflectometer (CS616-L40, Campbell Scientific), and the level of the water table is recorded with a pressure transducer (CS450-L, Campbell Scientific). At the time of the study, soil heat flux was not measured. Local meteorological variables are measured at a weather station approximately 1 km southeast of the tower, with a temperature/RH probe (HMP45C-L40, Vaisala, Woburn, MA, USA), a type-E fine-wire thermocouple, a cup anemometer (model 05103-L40, R.M. Young, Traverse City, MI, USA), a rain gage (TE525WS, Campbell Scientific), and a barometer (CS106, Vaisala).

Data are processed at the datalogger (CR5000, Campbell Scientific) for wind rotation, the Webb-Pearman_Leuning correction, and averaging (30 min intervals, for the dataset used in the current study). Raw and processed data are relayed to a nearby building by spread spectrum radio (RF450, Campbell Scientific) operating at 900 MHz. Records are transferred at intervals by Internet to the Texas A&M Agrilife Research and Extension Center at El Paso, TX, USA. The system is powered by a 70 W solar panel (SP20, Campbell

Scientific). Maintenance of all sensors is performed approximately monthly or when malfunctions are indicated.

3. Results and discussion

3.1. Quality and usability of eddy-covariance data

EC data are available for most of the interval between 3 June 2010 and 3 May 2011. We chose to analyze the data for July and August 2010 because the data quality was high, the canopy was fully developed and rather static in leaf characteristics, and the principal environmental drivers (insolation, air temperature, humidity, and wind speed) showed wide ranges that test model responses. As evidence of EC data quality, we present daily-total energy closure values in Supplementary Material (Part S1 and Fig. S1). Closure averages 92%, which is excellent in reference to FluxNet studies (Wilson et al., 2002; Leuning et al., 2012). Closure could not be evaluated during 4–15 August because of problems with the net radiometer. One concern with the EC data is that canopy cover varies with fetch direction. From aerial imagery, we quantified fractional cover along eight principal compass directions. Cover varied from 60% to 86%. However, averaged over the entire photoperiod on a daily basis, the effect was modest (Supplementary Material Part S2 and Fig. S2). In good part, this insensitivity resulted from relatively small variation in mean wind direction during July and August 2010. Furthermore, even the larger variations in cover did not explain the significant interdiel nor intradiel variations in fluxes (Supplementary Material Part S3 and Fig. S3).

3.2. Environmental responses evident in EC data and the model

Strong variation in the environmental drivers is apparent both within and between days (Supplementary Material, Part S4 and Fig. S4), which enables testing of canopy responses to diverse conditions. No one driver is highly dominant in determining fluxes, particularly of latent heat, *LE*, whether in the EC data or in the model simulations. Supplementary Material (Part S5 and Figures S5 and S6) show that daily-total shortwave insolation, Q_{sol}, has only a modest correlation with measured *LE* ($r^2 = 0.26$ including days of high advection, or 0.32 excluding these days), although the mean ratio of *LE* to Q_{sol} is high, at 0.63. The same weak correlation and low ratio of LE/Q_{sol} are apparent in the modeled LE ($r^2 = 0.37$). The slope of the regression is low, 0.34 to 0.46, depending upon whether one includes or excludes days of high advection of hot, dry air that drives high *LE*. The low slope is indicative of a rise in light-use efficiency in cloudy times; the relatively high ratio of stomatal conductance to Q_{sol} helps to support higher *LE*.

Fig. 2 shows that the model reproduced the patterns in the time series of *LE* well, other than on advective days. It also shows that the measured fluxes have large interdiel and intradiel variations; the season chosen for analysis presents a strong test of orchard responses to the environment. The time series of CO_2 flux (A_{can}) is also well-reproduced (Fig. 3), even on advective days. The model does show an earlier rise of photosynthetic flux at the beginning of the photoperiod; it is possible that the real canopy has a delay in activation of the rate-limiting Rubisco enzyme (Portis, 2003). The high *LE* fluxes in the EC measurements are linked to high canopy stomatal conductance, g_{can}, which the model in its basic form does not reproduce. However, stomata exert much less control over A_{can} than over *LE*. The control coefficients in Fig. 4 were estimated in the model as the relative increase in *E* (or A_{can}) divided by the relative increase in g_{can} (see Section 2.1.9). The time series for sensible heat flux is poorly represented in the model (Fig. 5), for yet-unclear reasons.

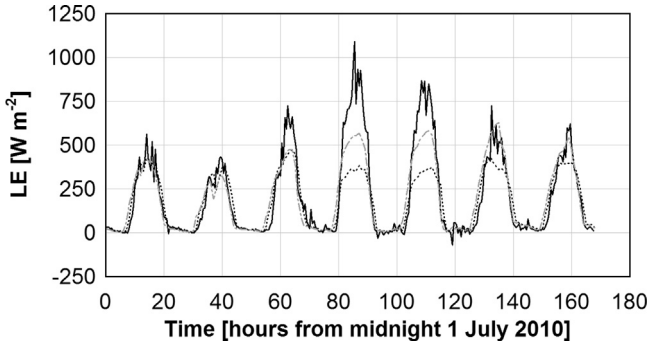

Fig. 2. Time series of latent heat flux for the first seven days of July 2010. Measured values (solid line) are half-hourly. Hourly values are modeled with the basic model (dashed line) or (dotted line) with a submodel of stomatal conductance having no sensitivity to humidity or *VPD*. Days 4 and 5 July have extreme advection of sensible heat into the canopy.

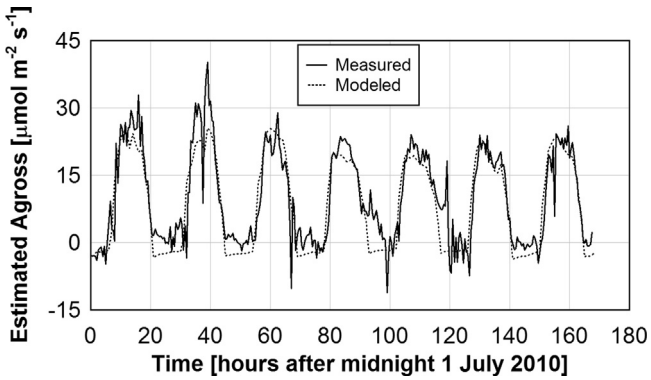

Fig. 3. Measured and modeled (dotted line) time series of gross CO_2 uptake for the first seven days of July 2010. Half-hourly values of eddy-covariance CO_2 fluxes (converted to the convention of positive flux as downward) are converted to gross uptake by subtracting estimated respiration from bole and soil. Modeled uptake is retained as an hourly series and includes only leaf respiration, not bole and soil respiration.

Further comparison of EC data with the model results is merited. The correlation of modeled and measured daily-total evapotranspiration (*ET*) is good, particularly when highly advective days are excluded (Fig. 6). More detailed comparisons of hourly values reveal shortcomings in the model's representation of processes. Fig. 7 shows the correlation between the model and the EC data. While the r^2 value is moderate, there is pronounced curvature in the relation, with the model producing overestimates at low *ET* and underestimates at high *ET* that is driven by high *VPD*. The Ball–Berry

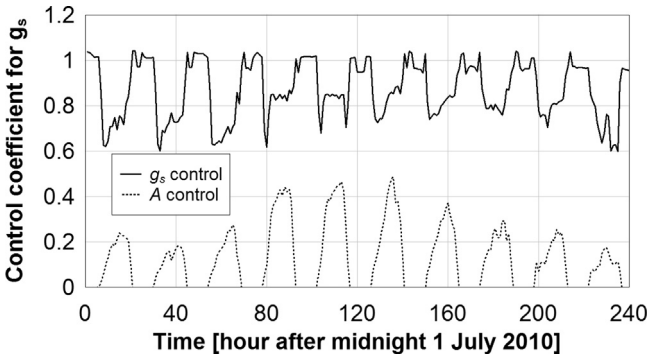

Fig. 4. Modeled values of control coefficients for stomatal conductance over transpiration (solid line) and photosynthetic rate (dotted line), for the first nine days of July 2010. Control over photosynthesis clearly vanishes in the dark. See Section 2 for the method of computing control coefficients.

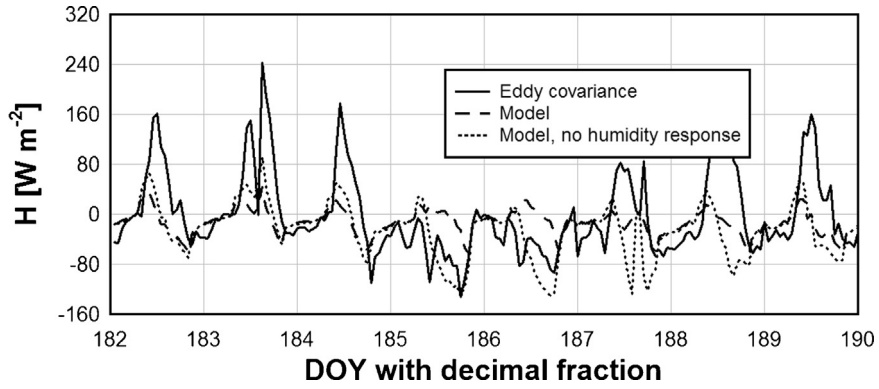

Fig. 5. Time series of hourly flux densities of sensible heat (H). The solid line is eddy-covariance data; the dashed line is flux simulated by the basic model, and the dotted line is flux simulated by the model with the humidity response turned off in the Ball–Berry model of stomatal conductance.

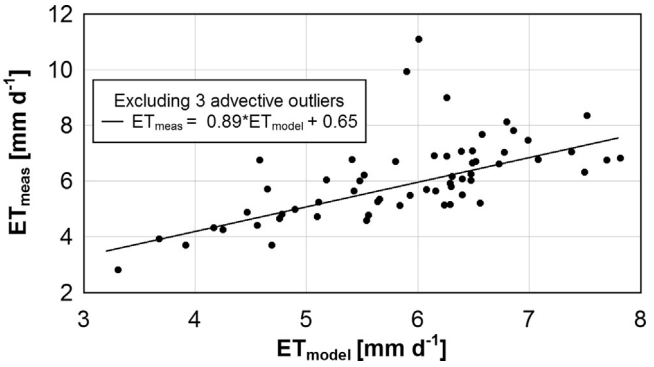

Fig. 6. Correlation of modeled daily-total ET with measured values, for all 62 days of the simulation. The straight line is the regression that excludes three days of extreme advection of sensible heat into the canopy (4 and 5 July, 7 August); $r^2 = 0.66$.

model of stomatal conductance may be responsible for the discrepancy, producing a strong reduction of g_s at high *VPD* (actually, at low relative humidity). Consequently, we progressively reduced the humidity response in the model, using a switch in the program that allows the user to set the exponent, generating a modified form, $g_s = m_{BB} A h_s^n / C_s + b_{BB}$. In order to account for the global mean value of h_s, it is then necessary to reset the value of m_{BB} from 10 to 4.65. Essentially, we are accounting for the mean value of h_s being approximately 0.5. With the exponent, n, reduced to zero (or 0.01, for mathematical stability of the solution method), the correlation of model and EC values increased markedly, to 0.86, as shown in Fig. 8. A non-response to humidity would make pecans very unusual, to be sure, but the strong increase of *ET* in hot, dry conditions appears to indicate such behavior. The data on stomatal conductance at the leaf level do not offer any significant support for nonresponsiveness to humidity. However, the data do not offer strong support for the contrary behavior. When the leaf gas-exchange data are fitted to a Ball–Berry model without a humidity response, the value of r^2 typically changes little, e.g., from 0.83 to 0.81. Together with the potential problems with slow equilibration of g_s that might not be achieved in the brief gas-exchange measurements, a very weak response of pecan leaves to humidity is plausible.

3.3. Finer resolution of canopy processes and their implications

Simplified models of crop productivity often use approximations that the photosynthetic rate is equal to light interception multiplied by a constant light-use efficiency (*LUE*). Similarly, these models assume a linear water production function (WPF), relating net photosynthesis linearly to water use (*ET*), possibly with a nonzero intercept. Models for irrigation management commonly relate daily-total *ET* to a reference *ET* computed with the simple Penman–Monteith model, which assumes a constant canopy conductance. Other models applicable to large land areas (e.g., the Surface Energy Balance Land model of Bastiaanssen et al., 1998) relate daily-total *ET* to remote-sensing estimates of *ET* at a single time of day, assuming a constant proportionality of *ET* to the reference *ET* at all times in the photoperiod. This method has been found empirically to give systematic underestimates (Ryu et al.,

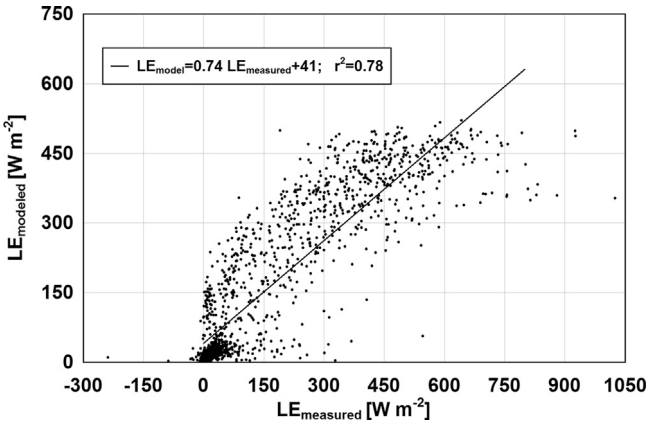

Fig. 7. Comparison of hourly latent heat fluxes, measured vs. modeled, for 59 days of the simulation, including three days of advective extremes. Half-hourly measured fluxes are aggregated into hourly values.

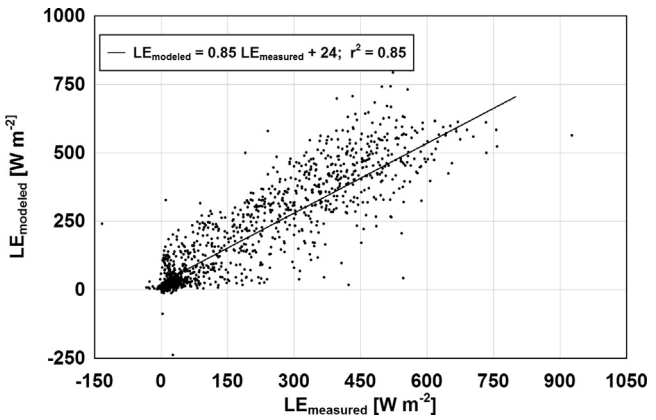

Fig. 8. Comparison of hourly latent heat fluxes, measured vs. modeled, for 59 days of the simulation, including 3 days of advective extremes. Simulation is as in Fig. 7, but with the humidity response turned off in the model of stomatal conductance.

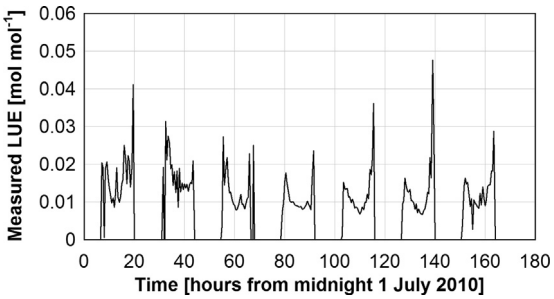

Fig. 9. Light-use efficiency variations measured by eddy covariance. Only the first seven days in July 2010 are shown, for clarity. *LUE* is computed as half-hourly net CO_2 uptake (mol m^{-2} s^{-1}) divided by PAR irradiance on a ground-area basis (mol m^{-2} s^{-1}) recorded at the weather station and aggregated to half-hourly totals.

2012); a process-based model such as ours may contribute to a firm theoretical method of scaling.

The fundamental enzyme kinetics of photosynthesis (e.g., Farquhar et al., 1980) militates against a value of *LUE* that is independent of light level or temperature. In the EC data, one sees that *LUE* varies within and between days (Fig. 9). Models of CO_2 and energy fluxes based on modified *LUE* are useful for large scales (Houborg et al., 2009) but with less accuracy than needed for orchard management. The model indicates an even stronger correlation, a strong decline of *LUE* with temperature (Supplementary Material Part S6 and Fig. S7). Further analysis shows that the truer correlation is with the amount of scattered light in the canopy (Supplementary Material Part S6 and Fig. S8). Scattered light rises with total light level; hence, it rises with higher solar elevations and higher air and canopy temperatures. A final investigation reveals that the model seriously overestimates scattered PAR flux density. At low solar elevations the model predicts that the fraction of scattered PAR substantially exceeds the approximate limit $1-a_{PAR} = 0.15$ (Supplementary Material Fig. S8; the limit is not firm, given that reflection from soil adds to total scattered light). The discrepancy is alleviated at moderate to high solar elevations. Better models of scattered light of all orders are needed. Most of the plausible alternative models, such as scattering between numerous discrete volume elements (Combes et al., 2008) or nested radiosity in an L-system model of canopy structure (*ibid.*), are computation-intensive. The stochastic model of Shabanov et al. (2007) may be useful but may have insufficient spatial resolution.

The model reports values of g_{can} that vary strongly within and between days (Fig. 10). It is notable that, with the humidity response of stomata turned off (dotted lines), g_{can} stays high on days of high advection, explaining the high LE values on these days. The EC data could not be processed to estimates of g_{can}, as there were no measurements of mean leaf temperature, $T_{leaf,avg}$. Such

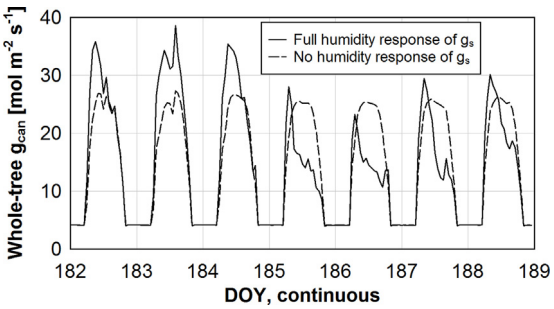

Fig. 10. Modeled large diurnal variations in total canopy conductance (g_{can}, stomata plus leaf boundary layer). Simulations are presented from the base model (solid line) or with humidity response turned off in the submodel of stomatal conductance (dotted line). Data are limited to first seven days of July for clarity. Conductance is the sum over all leaf area on the central tree.

measurements are needed in order to invert the (approximate) equation for whole-canopy transpiration, $E_{tree} = g_{can}(e_{sat}(T_{leaf,avg}) - e_{air,can})$. While the inconstancy of g_{can} is not a new finding, being apparent in empirical measurements in a number of other studies (e.g., Kochendorfer et al., 2011), our model resolves the complex processes that generate this behavior. This process resolution may be expected to aid in developing simpler models that are largely consistent with actual complex behavior.

By tracking many individual processes such as light interception, our model facilitates estimation of contributions of various processes to final fluxes. In particular, it reports histograms of leaf irradiance, I_{leaf}, leaf temperature, T_{leaf}, leaf transpiration, E_{leaf}, leaf photosynthetic rate, A_{leaf}, leaf total conductance (through stomata plus the boundary layer), $g_{tot,leaf}$, and various weighted values, such as transpiration-weighted leaf irradiance or photosynthetic-rate-weighted leaf temperature. The histogram of raw leaf irradiance at 3 PM (a time of peak E and A) (Supplementary Material Part S7 and Fig. S9) is readily analyzed to sunlit leaf area by extrapolating the long tail of high irradiance back to the minimal value and integrating the area. It shows that sunlit leaf area comprises 46% of total leaf area in the model. Supplementary Material Figure S9 also shows the histogram of photosynthesis-weighted irradiance, which, by a similar analysis, predicts that sunlit leaf area performs 75% of net leaf photosynthesis in the whole tree. Thus, it performs at a mean rate that is (75/46)/(25/54) = 3.5 times greater than shaded leaf area. A similar value obtains for the contribution of sunlit leaf area to transpiration and to total canopy conductance (figures not shown, for brevity). Predicted leaf temperatures are shown in Supplementary Material Part S8 and Fig. S10. Shaded leaf area clumps at low leaf temperatures, as expected, while sunlit leaf area extends to values about 4 °C higher. Supplementary Material Part S9 and Fig. S11 presents the modeled histogram of leaf photosynthetic rate, A_{leaf}. There is a large peak at low values from shade leaves and a broad peak at intermediate to high values from sunlit leaves, trailing off strongly at the highest values from light saturation.

4. Conclusions

The ultimate use of the model is twofold, in developing decision support systems for field practices and in improving the understanding of physiological and biophysical processes that determine ultimate performance of pecans and similar tree crops. The performance of the model against field data obtained with eddy covariance is a test of the utility of the model at these two levels.

First and foremost as a test is evaluating the model's accuracy for its ultimate use in developing decision support systems that apply broadly across climatic regimes, tree varieties, and orchard management practices that include irrigation, mineral nutrient fertilization, tree spacing, and pruning. For such use, a process-based model gives a sound basis, in that directly measurable meteorological conditions, physiological condition, and canopy structure can be used, obviating empirical fitting that has limited guidance in field practice without extensive and costly or impractical experimentation. By this criterion, the model demonstrates a quite encouraging degree of success in predicting responses of evapotranspiration and canopy photosynthetic rate to meteorological drivers, physiological parameters, and canopy structure. The correlation of the model to field data for sensible heat flux is more problematic and currently unexplained. One remarkable inference of the modeling study is that pecan stomatal conductance may be very insensitive to humidity or vapor-pressure deficit. This limited test merits further field research at levels from leaf to canopy.

In the current study, the model has only been tested in mid-season under high levels of water availability and fertilizer use.

The present model already incorporates responses to water stress, though field tests of these responses are sparse to date. More testing is merited at other levels of water and N. Additionally, the model's high resolution of processes or high dimensionality must be projected to lower levels in order to generate a decision support system, which is an effort for subsequent research. The model, which does not allocate growth and use of carbohydrates and nutrients, must be coupled to a larger model. Concurrent research (Sammis et al., 2013) does address the development of leaf area, transition to nutfill, nutrient relations, and other processes occurring over whole seasons. There remains a variety of limitations in the model to be addressed in future research. These limitations include inadequate accounting for soil-surface energy balance (only shortwave radiative balance is used currently), approximations in accounting for scattered radiation in the canopy, and perhaps the assumption of full activation in the entire photoperiod of Rubisco as a potentially rate-limiting enzyme for photosynthesis. The last approximation may account for the model predicting a too-early rise of photosynthetic rate near dawn.

Second, and equally relevant to another research community, is the level of success in reproducing diverse biophysical and physiological processes contributing to the water and CO_2 fluxes and the known couplings among these processes. The model shows that no one meteorological driver, not even total insolation, explains the majority of the variance in ET. The violation by the model of limits on light-use efficiency at low solar elevation highlights the need for better but still simple models of scattered light in highly structured plant canopies.

Both the model and the eddy-covariance data show that canopy conductance and light-use efficiency vary considerably over the day and between days. These findings affirm that the use of simple models such as Penman–Monteith with constant canopy conductance for reference ET and thus for irrigation management introduces inaccuracies. The same can be said for simple light-use efficiency models for crop productivity. Of course, there are empirical adjustments, such as using statistical correlations of canopy conductance with hourly meteorological variables (e.g., Allen et al., 1998, for the FAO programs). However, the empirical adjustments demand calibration to plant species, variety, and local conditions of climate and soil. The simple models offer no guidance to performance of crops under water or nitrogen stresses that are expected to become much more common under new regimes of water availability enforced by climate change, rising energy costs, and increasing competition of various water uses with agriculture. A process-based model such as presented here may be more accurate to use in the long term, particularly if there are robust patterns in plant parameters. An example is the near-constancy of the Ball-Berry slope in representing the control of stomatal conductance (Gutschick and Simonneau, 2002). It is well worth exploring, in future research, the sensitivity of predicted fluxes and water-use efficiency to changes in (errors in) model input parameters. We have seen in a few tests here that ET scales only modestly with foliage density or with leaf maximal carboxylation capacity, as near power laws with relatively low power (<0.5). This favors using more rapid if somewhat crude estimates for a number of model parameters.

The model resolves some processes that are poorly amenable to direct measurement. These include the histograms of leaf performance conditions, such as the distribution of PAR irradiance levels, with or without weighting by factors such as leaf temperature. The PAR irradiance histograms reveal, under the assumptions of the radiative transfer submodel, that it is quite important to resolve the full range of irradiances rather than to use simple models that assign leaves as either shaded or sunlit at a single, average irradiance. It appears to be moderately important to account for the interception of relatively "cool" sky thermal radiation at diverse levels at various points in the canopy, in order to get accurate estimates of leaf energy balance, hence, of ET and photosynthetic rates.

Finally, the model is ready for initial predictions of the effects of substantial levels of water stress on the water use and productivity of pecans–and, with some modification, of other tree crops. The predictions could identify the most sensitive drivers of yield impacts and the most sensitive indicators of impact. Thus, use of a sufficiently well-verified model can reduce the number of field tests needed, which tests are expensive and risky to a valuable perennial crop.

Acknowledgements

The authors wish to thank Theodore W. Sammis of New Mexico State University for critical reviews of the research and of the manuscript, as well as for facilitating funding for the research of author Gutschick. They also thank Jose Ernesto Frias-Ramirez of the Instituto Tecnológico De Torreón and Ernesto A. Catalan-Valencia of the Universidad Juárez del Estado de Durango for contributing to the initial development of the model, Tony Rancich for the use of his commercial orchard, the Sonic Ranch, orchard manager Alfredo Sanchez for access to facilities and for logistics, and research technician Ricardo S. Marmolejo of the Texas A&M AgriLife Research and Extension Center for installation and operation of the eddy-covariance system. Reyes Duran assisted with the editing of this manuscript. The research of author Gutschick was supported by the USDA Specialty Crops Program, the New Mexico Agricultural Experiment Station. The research of author Sheng was supported in part by the Rio Grande Basin Initiative, which is administrated by Texas Water Resources Institute and sponsored by the National Institute of Food and Agriculture, U.S. Department of Agriculture, under Agreement Numbers 2010-34461-20677.

Appendix A.

A.1. Decomposing pyranometer data into estimates of PAR vs. NIR and of direct beam vs. diffuse skylight

The model assumes that the PAR and NIR energy flux densities are equal. Both of these fluxes must then be decomposed into the above-canopy direct-beam flux density, I_0, and the diffuse flux density, D_0. The model computes the solar zenith and azimuthal angles for the latitude, longitude, Julian day, and local civil time (Roderick, 2004). From the solar elevation, it computes the expected direct plus diffuse energy flux density on a horizontal surface for a clear sky and known air mass. Shortfalls from the expected value are attributed to partial cloudiness, to adjust the values of both I_0 and D_0. Full details are given in the comments embedded in the code.

A.2. Soil-to-root hydraulic resistance

The water movement from bulk soil to fine root surfaces driven by transpiration generates a drop in water potential between soil and root, $\psi_{soil} - \psi_{root} = R_{soil} E_{tree}$. Assuming steady state in a cylindrically symmetric geometry at each root, $R_{soil} = C\, \rho_{root}\, r_{root}^2\, ln(d/r_{root})/(2^* m_{root}\, k_h)$. This expression is readily derived and is similar to that in Lafolie et al. (1991). Here, C is a factor correcting for root clumping that reduces water extraction (Tardieu et al., 1992); ρ_{root} is the fine-root dry-mass density; r_{root} is the mean radius of fine roots; d is the mean spacing between fine roots; m_{root} is the whole-tree mass of fine roots; and k_h is the hydraulic conductivity of soil in metric units of Pa m^{-1}. The root spacing is computed from root-length density, $d = 1/\sqrt{RLD}$, and RLD is computed from the total root length as distributed throughout the volume

composed by the soil depth and the ground area per tree. The hydraulic conductivity is computed at any soil water potential using the form of van Genuchten (1980).

A.3. Stabilization of iteration of water potentials and transpiration rate

Whole-tree transpiration rate, E_{tree}, can change markedly between hours of the simulation, inducing significant changes in leaf water potential, ψ_{leaf}. By the reasonably realistic model of stomatal conductance, this signal causes a reduction in stomatal conductance at all leaves, hence, a reduction in E_{tree} itself. The reduction in E_{tree}, in turn, can predict an increase in stomatal conductance and an increased E_{tree} in the next iteration. The oscillations between iterations of E_{tree} can prevent convergence of the solution. We found a method of stabilization.

In our model, the expression for stomatal conductance as affected by water potentials can be written as $g_s = g_s^0 \exp(\beta\psi_{root} + \delta\psi_{leaf}) = f_{gs} g_s^0$, where $g_s{}^0$ is the Ball–Berry form responsive only to the aerial environment, ψ_{root} is the root water potential, ψ_{leaf} is the leaf water potential, and β and δ are empirical coefficients. Now, both water potentials are related to the soil water potential, ψ_{soil}, which is rather stable between time steps, and to the whole-tree transpiration rate, E_{tree}, and two hydraulic resistances, R_{soil} from bulk soil to root surfaces and R_{stem} from roots to leaves. Given the relations that $\psi_{root} = \psi_{soil} - R_{soil}\ E_{tree}$ and $\psi_{leaf} = \psi_{root} = R_{stem}\ E_{tree}$, we can write the argument of the exponential as $(\beta+\delta)\psi_{soil} - (\beta R_{soil} + \delta[R_{soil} + R_{stem}])\ E_{tree} = A - B\ E_{tree}$. We can then compute a factor by which transpiration is cut by water stress, writing $E_{tree} = E_0 \exp(-B\ E_{tree})$. Here, E_0 is the rate driven by the aerial environment and the soil water potential and B is the factor in the second parentheses. This is a transcendental equation in E_{tree}, which we can solve by Newton–Raphson iteration. We construct an initial estimate of E_{tree} as the mean of the previous hour's value of E_{tree} and the most recent iteration this hour. The iterative changes in E_{tree} are hobbled, reduced to 0.7 of their computed value, to prevent oscillations. The solutions always converge.

A.4. Foliage density

Foliage density in a pecan canopy is a function of age and nutrition, among other factors, and in most commercial orchards it achieves similar values. A quick estimate can be made from the fractional penetration of direct sunlight to the ground. This estimate uses the relation $P_{pen} = \exp(-0.5^{*}L)$ for a uniform leaf-angle distribution, with L = mean leaf area index across the crown = $(4/3)\pi R^3 f_d / \pi R^2 = (4/3) R f_d$, where R is the radius of the crown. (This formula is not exact for a spherical crown.) Photographs indicated 16% penetration within the crown shadow, yielding $L = 3.67$. For a crown radius of 4.25 m, f_d then takes the value 0.65 m^{-1}. A more sophisticated model that takes account of the variation of effective leaf area index radially from the center gives the value $f_d = 0.75\ m^{-1}$, under the assumption that foliage density is uniform even through the center of the tree, which is not the case. One question in modeling is, How sensitive are the results to the accuracy of estimation of foliage density? We ran simulations with foliage density shifted from 0.65 m^{-1} to 0.55 or 0.75 in the same units, that is, up or down by 16%. The relative change in whole-tree transpiration was 7%; an offset or error in f_d propagated about 44% as large an error, relatively, in transpiration. That is, transpiration scales less than linearly with f_d, and even less than as the square root. Thus, mean foliage density is moderately important to know accurately. In other simulations, we found that the model results were equally sensitive to errors in leaf carboxylation capacity and more sensitive to the value of the Ball–Berry slope.

If we allow foliage density to increase exponentially from the center by a factor of 3, for example, we may set the central foliage density to 0.3 m^{-1}. By numerical integrations, this gives a mean foliage density of 0.70 m^{-1} in the whole canopy and 15.8% penetration across the crown. This agrees well with values that we used. Of course, such a radially-dependent foliage density would alter the sunlit fraction of leaves. A uniform canopy with the same mean foliage density has a penetration fraction of 17.6%; there is less clumping of leaf area along paths through the crown with high column leaf area index. More realistic models of foliage distribution are merited.

A.5. Leaf physiological parameters

We reanalyzed the leaf gas-exchange data of Johnson (2004) to estimate the stomatal control parameters m_{BB} and b_{BB} and the maximal carboxylation capacity $V_{c,max}{}^{25}$. The gas-exchange system, a LI-COR LI-6400, reported the net photosynthetic rate of the leaf, A_{leaf}, the stomatal conductance, g_s, the leaf-interior CO_2 mixing ratio, the leaf temperature, T_{leaf}, and the values in cuvette air of the total air pressure, the partial pressure of water vapor, and the mole fraction of CO_2. From these data we could compute the relative humidty, h_s, and the CO_2 mixing ratio, C_s, at the leaf surface, in order to compose the Ball–Berry index, $I_{BB} = A_{leaf}\ h_s / C_s$. The index varied over the course of any morning's measurements on typically tens of measurements on (different) leaves. Assuming that the leaves are physiologically similar (leaves with good exposure to sunlight on the edge of the crown), we obtained m_{BB} and b_{BB} from linear regressions of g_s against the index I_{BB}. We could also estimate carboxylation capacity by inverting the expression of Farquhar et al. (1980) for the carboxylation-limited photosynthetic rate. This is an effective value, because one should use the CO_2 partial pressure at the chloroplast, which is lower.

We believe that the mean carboxylation capacity is estimated well by restricting the sample to leaves that began at high PAR irradiance and were thus fully activated. On the contrary, the Ball–Berry parameters were less accurately estimated because the leaves were often put into environmental conditions in the cuvette that differed significantly from the free-air initial conditions. Stomata of tree leaves tend to have response times of many minutes, longer than the typical 2 min for the measurements done by Johnson (2004). The Ball–Berry parameters were obtained more reliably in the work of Frias-Ramirez (2002) and their means were 10 and 0.02 mol m^{-2} s^{-1}. These values are similar to those for many other plants (Gutschick and Simonneau, 2002).

A.6. Soil and root descriptors

The parameters for the leaf water-stress response, β and δ, are set at 0.283 and 0.216 MPa^{-1}, and the stem hydraulic resistance is set at 0.01 MPa (L h^{-1}), based on limited observations of root-to-leaf reductions in water potential in mature trees by Johnson (2004). Soil type is set as clay loam, as observed, and the values of parameters for the soil-moisture release curve are taken from Hodnett and Tomasella (2002) and for soil hydraulic conductivity from van Genuchten (1980). Soil depth was artificially set to 3 m in the current study as a simple method to minimize water depletion and attendant water stress, without implementing a more complex scheme of accounting for (fully sufficient) irrigation. Per-tree fine root mass of 95 kg and mean fine-root radius of 0.001 m are taken from studies by Sammis et al. (2013).

Appendix B. Supplementary data

Supplementary data associated with this article can be found, in the online version, at http://dx.doi.org/10.1016/j.agwat.2013.08.004.

References

Allen, R.G., Pereira, L.S., Raes, D., Smith, M., 1998. Crop Evapotranspiration: Guidelines for Computing Crop Water Requirements. FAO Irrigation and Drainage, Rome, 300 pp.

Andales, A., Wang, J., Sammis, T.W., Mexal, J.G., Simmons, L.J., Miller, D.R., Gutschick, V.P., 2006. A model of pecan growth for the management of pruning and irrigation. Agric. Water Manage. 84, 77–88.

Baldocchi, D., 1997. Flux footprints within and over forest canopies. Boundary-Layer Meteorol. 85, 273–292.

Ball, J.T., Woodrow, I.E., Berry, J.A., 1987. A model predicting stomatal conductance and its contribution to the control of photosynthesis under different environmental conditions. In: Biggins, J. (Ed.), Progress in Photosynthesis Research, vol. 4. M. Nijhoff Publishers, Dordrecht, pp. 221–224.

Barr, A.G., Morgenstern, K., Black, T.A., McCaughey, J.H., Nesic, Z., 2006. Surface energy balance closure by the eddy-covariance method above three boreal forest stands and implications for the measurement of CO_2 flux. Agric. For. Meteorol. 140, 322–337.

Bastiaanssen, W.G.M., Menenti, M., Feddes, R.A., Holtslag, A.A.M., 1998. A remote sensing surface energy balance algorithm for Land (SEBAL), Part 1: Formulation. J. Hydrol. 212–213, 198–212.

Behboudian, M.H., Mills, T.M., 1997. Deficit irrigation in deciduous orchards. Hort. Rev. 21, 105–131.

Brutsaert, W., 1975. On a derivable formula for long-wave radiation from clear skies. Water Resour. Res. 11, 742–744.

Buckley, T.N., 2005. The control of stomata by water balance. New Phytol. 168, 275–292.

Campbell, G.S., Norman, J.M., 1998. An Introduction to Environmental Biophysics, second ed. Springer, New York.

Cochard, H., Coll, L., Le Roux, X., Ameglio, T., 2002. Unraveling the effects of plant hydraulics on stomatal closure during water stress in walnut. Plant Physiol. 128, 282–290.

Combes, D., Chelle, M., Sinoquet, H., Varlet-Grancher, C., 2008. Evaluation of a turbid medium model to simulate light interception by walnut trees (hybrid NG38× RA and *Juglans regia*) and sorghum canopies (*Sorghum bicolor*) at three spatial scales. Funct. Plant Biol. 35, 823–836.

Deb, S.K., Shukla, M.K., Mexal, J.G., 2011. Numerical modeling of water fluxes in the root zone of a mature pecan orchard. Soil Sci. Soc. Am J. 75, 1667–1680.

Dewar, R.C., 2002. The Ball–Berry–Leuning and Tardieu–Davies stomatal models: synthesis and extension within a spatially aggregated picture of guard cell function. Plant, Cell Environ. 25, 1383–1398.

Farquhar, G.D., von Caemmerer, S., Berry, J.A., 1980. A biochemical model of photosynthetic CO_2 assimilation in leaves of C_3 species. Planta 149, 78–90.

Fernandez, J.E., Diaz-Espejo, A., Infante, J.M., Duran, P., Palomo, M.J., Chamorro, V., Giron, I.F., Villagarcia, L., 2006. Water relations and gas exchange in olive trees under regulated deficit irrigation and partial rootzone drying. Plant Soil 284, 273–291.

Frias-Ramirez, J.E., 2002. Physiological Model of Light Interception and Water Use in Pecan Trees. New Mexico State University, Las Cruces, NM, USA (PhD dissertation).

Fye, R.E., Reddy, V.R., Baker, D.N., 1981. Cotton Plants—A Preliminary GOSSYM Model. Science Education Admin Publications AAT, Oakland, pp. 1–36.

Gijon, M.C., Guerrero, J., Couceiro, J.F., Moriana, A., 2009. Deficit irrigation without reducing yield or nut splitting in pistachio (*Pistacia vera* cv Kerman on *Pistacia terebinthus* L.). Agri. Water Manage. 96, 12–22.

Goldhamer, D.A., Fereres, E., 2004. Irrigation scheduling of almond trees with trunk diameter sensors. Irrig. Sci. 23, 11–19.

Gutschick, V.P., 1988. Statistical penetration of diffuse light into vegetative canopies—effect on photosynthetic rate and utility for canopy measurement. Agric. Meteorol. 30, 327–341.

Gutschick, V.P., 1991. Joining leaf photosynthesis models and canopy photon-transport models. In: Myneni, R.B., Ross, J. (Eds.), Photon-Vegetation Interactions: Applications in Optical Remote Sensing and Plant Ecology. Springer-Verlag, Berlin, Germany, pp. 501–535.

Gutschick, V.P., Simonneau, Th., 2002. Modelling stomatal conductance of field-grown sunflower under varying soil water content and leaf environment: comparison of three models of stomatal response to leaf environment and coupling with an abscisic acid-based model of stomatal response to soil drying. Plant Cell Environ. 25, 1423–1434.

Hodnett, M.G., Tomasella, J., 2002. Marked differences between van Genuchten soil water-retention parameters for temperate and tropical soils: a new water-retention pedo-transfer functions developed for tropical soils. Geoderma 108, 155–180.

Houborg, R., Anderson, M.C., Norman, J.M., Wilson, T., Meyers, T., 2009. Intercomparison of a 'bottom-up' and 'top-down' modeling paradigm for estimating carbon and energy fluxes over a variety of vegetative regimes across the U.S. Agric. For. Meteorol. 149, 1875–1895.

Johnson, D.C., 2004. Prediction of Water Stress in Pecan Orchards with Remote Sensing. New Mexico State University, Las Cruces, NM, USA (MS thesis).

Johnson, I.R., 2011. Testing and evaluating large-scale agricultural simulation models. In: 19th International Conference on Modelling and Simulation, Perth, Australia, 12–16 December.

Kallestad, J.C., Sammis, T.W., Mexal, J.G., White, J., 2006. Monitoring and management of pecan orchard irrigation: a case study. Hort. Technol. 16, 667–673.

Kochendorfer, J., Castillo, E.G., Haas, E., Oechel, W.C., Paw, U.K.T., 2011. Net ecosystem exchange, evapotranspiration and canopy conductance in a riparian forest. Agric. For. Meteorol. 151, 544–553.

Lafolie, F., Bruckler, L., Tardieu, F., 1991. Modeling root water potential and soil-root water transport: I. Model presentation. Soil Sci. Soc. Am. J. 55, 1203–1212.

Leuning, R., 1995. A critical appraisal of a combined stomatal-photosynthesis model for C_3 plants. Plant Cell Environ. 18, 339–355.

Leuning, R., van Gorsel, E., Massman, W.J., Isaac, P.R., 2012. Reflections on the surface energy imbalance problem. Agric. For. Meteorol. 156, 65–74.

Liang, S., Strahler, A.H., 1995. An analytic radiative transfer model for a coupled atmosphere and leaf canopy. J. Geophys. Res. D: Atmos. 100, 5085–5094.

Lombardini, L., Restrepo-Diaz, H., Volder, A., 2009. Photosynthetic light response and epidermal characteristics of sun and shade pecan leaves. J. Amer. Soc. Hort. Sci. 134, 372–378.

Matthews, K.B., Schwarz, G., Buchan, K., Rivington, M., 2008. Wither agricultural DSS? Comput. Electron. Agric. 61, 149–159.

Matzner, S., Comstock, J., 2001. The temperature dependence of shoot hydraulic resistance: implications for stomatal behaviour and hydraulic limitation. Plant Cell Environ. 24, 1299–1307.

Miyamoto, S., 1984. A model for scheduling pecan irrigation with microcomputers. Trans. ASABE. 27, 456–463.

Niinemets, Ü., 2007. Photosynthesis and resource distribution through plant canopies. Plant Cell Environ. 30, 1052–1071.

Portis, A.R., 2003. Rubisco activase—Rubisco's catalytic chaperone. Photosynth. Res. 75, 11–27.

Ribas-Carbo, M., Taylor, N.L., Giles, L., Busquets, S., Finnegan, P.M., Day, D.A., Lambers, H., Medranao, H., Berry, J.A., Flexas, J., 2005. Effects of water stress on respiration in soybean leaves. Plant Physiol. 139, 466–473.

Roderick, M.L., 2004. Methods for calculating solar position and day length including computer programs and subroutines. In: Resource Management Technical Report No. 137, Western Australia Dept. of Agriculture, South Perth, WA.

Romero, P., Garcia, J., Botia, P., 2005. Cost-benefit analysis of a regulated deficit-irrigated almond orchard under subsurface drip irrigation conditions in South-eastern Spain. Irrig. Sci. 24, http://dx.doi.org/10.1007/s00271-005-0008-6.

Ross, J., 1981. The Radiation Regime and Architecture of Plant Stands. Dr. W. Junk, The Hague.

Ryu, Y., Baldocchi, D.D., Black, T.A., Detto, M., Law, B.E., Leuning, R., Miyata, A., Reichstein, M., Vargas, R., Ammann, C., Beringer, J., Flanagan, L.B., Gu, L., Hutley, L.B., Kim, J., McCaughey, H., Moors, E.J., Rambal, S., Vesala, T., 2012. On the temporal upscaling of evapotranspiration from instantaneous remote sensing measurements to 8-day mean daily-sums. Agric. For. Meteorol. 152, 212–222.

Sammis, T.E., Gutschick, V.P., Wang, J., Miller, D.R., 2013. Model of water and nitrogen management in pecan trees under normal and resource-limited conditions. Agric. Water Manag. 124, 28–36.

Schmid, H.P., 2002. Footprint modeling for vegetation atmosphere exchange studies: a review and perspective. Agric. For. Meteorol. 113, 159–183.

Sellers, P.J., Randall, D.A., Collatz, G.J., Field, C.B., Dazlich, D.A., Zhang, C., Collelo, G.D., Bounoua, L., 1996. A revised land surface parameterization (SiB2) for atmospheric GCMs. Part I: model formulation. J. Clim. 9, 676–705.

Shabanov, N.V., Huang, D., Knjazikhin, Y., Dickinson, R.E., Myneni, R.B., 2007. Stochastic radiative transfer model for mixture of discontinuous vegetation canopies. J. Quant. Spectrosc. Radiat. Transfer. 107, 236–262.

Shackel, K.A., Lampinen, B., Southwick, S., Olson, W., Sibbett, S., Krueger, W., Yeager, J., 2000. Deficit irrigation in prunes: maintaining productivity with less water. Hort. Sci. 35, 1063–1066.

Tardieu, F., Simonneau, Th., 1998. Variability among species of stomatal control under fluctuating soil water status and evaporative demand: modelling isohydric and anisohydric behaviours. J. Exp. Bot. 49, 419–432 (special issue).

Tardieu, F., Bruckler, L., Lafolie, F., 1992. Root clumping may affect the root water potential and the resistance to soil-root water transport. Plant Soil 140, 291–301.

Thomas, D.S., Eamus, D., 2002. Seasonal patterns of xylem sap pH, xylem abscisic acid concentration, leaf water potential and stomatal conductance of six evergreen and deciduous Australian savanna tree species. Aust. J. Bot. 50, 229–236.

van Genuchten, M.Th., 1980. A closed-form equation for predicting the hydraulic conductivity of unsaturated soils. Soil Sci. Soc. Am. J. 44, 892–898.

Vogel, C.A., Baldocchi, D.D., Luhar, A.K., Rao, K.S., 1995. A comparison of a hierarchy of models for determining energy-balance components over vegetation canopies. J. Appl. Meteorol. 34, 2182–2196.

Vörösmarty, C.J., McIntyre, P.B., Gessner, M.O., Dudgeon, D., Prusevich, A., Green, P., Glidden, S., Bunn, S.E., Sullivan, C.A., Reidy Liermann, C., Davies, P.M., 2010. Global threats to human water security and river biodiversity. Nature 467, 555–561.

Wada, Y., van Beek, L.P.H., Bierkens, M.F.P., 2012. Nonsustainable groundwater sustaining irrigation: a global assessment. Water Resour. Res. 48, http://dx.doi.org/10.1029/2011WR010562.

Wang, J.M., Sammis, T.W., Andales, A.A., Simmons, L.J., Gutschick, V.P., Miller, D.R., 2007. Crop coefficients of open-canopy pecan orchards. Agric. Water Manage. 88, 253–262.

Wilkerson, G.G., Jones, J.W., Boote, K.J., Ingram, K.T., Mishoe, J.W., 1983. Modeling soybean growth for crop management. Trans. ASABE 26, 63–73.

Wilson, K.B., Baldocchi, D.D., Hanson, P.J., 2000. Quantifying stomatal and non-stomatal limitations to carbon assimilation resulting from leaf aging and drought in mature deciduous tree species. Tree Physiol. 20, 787–797.

Wilson, K., Goldstein, A., Falge, E., Aubinet, M., Baldocchi, D., Berbiger, P., Bernhofer, C., Ceulemans, R., Dolman, H., Field, C., Grelle, A., Ibrom, A., Law, B.E., Kowalski, A., Meyers, T., Moncrieff, J., Monson, R., Oechel, W., Tenhunen, J., Valentini, R., Verma, S., 2002. Energy balance closure at FLUXNET sites. Agric. For. Meteorol. 113, 223–243.

Wythers, K.R., Reich, P.B., Tjoelker, M.G., Bolstad, P.B., 2005. Foliar respiration acclimation to temperature and temperature variable Q_{10} alter ecosystem carbon balance. Glob. Change Biol. 11, 435–449.